Exhibit C

CW370 USER MANUAL

Table of Contents

Dynamic Light Scattering Theory

Introduction

In recent years, the technique of dynamic light scattering (DLS) -- also called quasi-elastic light scattering (QELS) or photon correlation spectroscopy (PCS) -- has proven to be an invaluable -analytical tool for characterizing the size distribution of particles suspended in a solvent (usually water). The useful size range for the DLS technique is quite large -from below 5 am (0.005 micron) to several microns. The power of the technology is most apparent when applied to the difficult Particularly for diameters below 300 nm submicron size range, where most competing measurement techniques lose their effectiveness or fail altogether. Consequently, DLS-based sizing instruments have been used extensively to characterize a wide range of particulate systems, including synthetic polymers (e.g. latexes, PVCs, etc.), oil-in-water and water-in-oil emulsions, vesicles, micelles, biological macromolecules, pigments, dyes, silicas, metallic sols, ceramics and numerous other colloidal suspensions and dispersions.

As we shall see, the DLS technique possesses a number of unique characteristics, which make it a powerful and effective tool for particle size analysis in the submicron region. Precisely because of the nature of some of these characteristics, a DLS instrument behaves like no other competing technology. Often, it will yield results of great accuracy, with excellent reproducibility. At other times, the results may be substantially distorted, and even misleading. In short, the "rules of the game" by which a DLS instrument operates result not only in distinct advantages, but also in potentially serious shortcomings, or pitfalls. It is the purpose of this section to provide insight into the scientific rationale for this technique, in general, and the NICOMP 370, in particular. In so doing, we hope to help maximize the use of the 370 and to become better prepared to ask the right kinds of questions whenever unexpected results occur. Our philosophy -- keep it simple! We have no intention of intimidating with a rigorous discussion of the physical principles of coherent light scattering or the detailed mathematics of Laplace transform inversion -- both of which figure prominently in the NICOMP 370. However, we do feel it useful to provide a reasonable review of the principles underlying the DLS technique. For the weak of heart -- skip directly to the section, The Simplest Approach to Size Distribution Analysis: Gaussian Analysis.

The Simplest Approach to Size Distributions: Gaussian Analysis

We shall see that two very different mathematical procedures, or "algorithms", have been developed to analyze the autocorrelation "raw data", C(t'), depending on the nature of the underlying particle size distribution. The Model 370 automatically selects the more appropriate of the two analysis procedures and provides the user with a running measure of the accuracy, or "goodness of fit", of the computed distribution resulting from the particular analysis chosen. Nevertheless, we feel it essential to gain an appreciation of the rationale behind each of the analysis methods and to become comfortable with some typical results obtained for actual particle systems. The latter can be studied in a controlled, accurate way using polystyrene latexes, oil-in-water emulsions and other well-characterized materials.

Broad unimodal distribution -- Gaussian Analysis

Following the discussion in the previous section, it is now obvious that a mixture of particle sizes must give rise to an autocorrelation function C(t') which decaying exponential function is *no longer* a simple i.e. having a single, well-defined decay time constant τ, as shown in Figure 8c. The existence of more than one rate of diffusion must necessarily give rise to a mixture of decaying exponential functions, each of which has a different time decay constant τ_i, corresponding to a particular diffusivity D_i and, hence, of particle radius R_i. The challenge which we face is to develop fast and efficient mathematical methods of analysis, whereby we can "deconvolve" C(t') and thereby extract the distribution of D values (and hence of particle diameters) from the detailed shape of C(t'). The "magic" behind the Model 370 has to do with its ability to obtain, accurately and consistently, the most useful information relating to the distribution of particle sizes in solution. To do this, the 370 must analyze precisely the deviations of autocorrelation function C(t') from single-exponential behavior. As we shall discover below, these deviations are often surprisingly slight and subtle, given the large range of complicated distributions which are encountered.

The Simplest Approach to Size Distributions: Gaussian Analysis

The simplest kind of complexity in the particle size distribution which we can introduce is a smooth, gaussian-like population of sizes, having a well-defined mean diameter and half width. Such an idealized distribution shape is often obtained for *emulsions*, prepared by a variety of processes, sonication, homogenization and microfluidization™. Typically, some type of oil and water are caused to be mixed together with the aid of a dispersing agent (e.g. a non-ionic surfactant) to form a single, microscopically homogeneous phase. The result: tiny droplets of one component (e.g. the oil) suspended in the other component, or "phase" (e.g. water). The mean size and width of the resulting droplet distribution are usually sensitive functions of the stoichiometry of the starting compounds and the duration and detailed nature of the preparation technique employed. In Figure 9a we show the autocorrelation function for a fat emulsion, used for intravenous ("IV") feeding. The channel width used here was 21 usec.

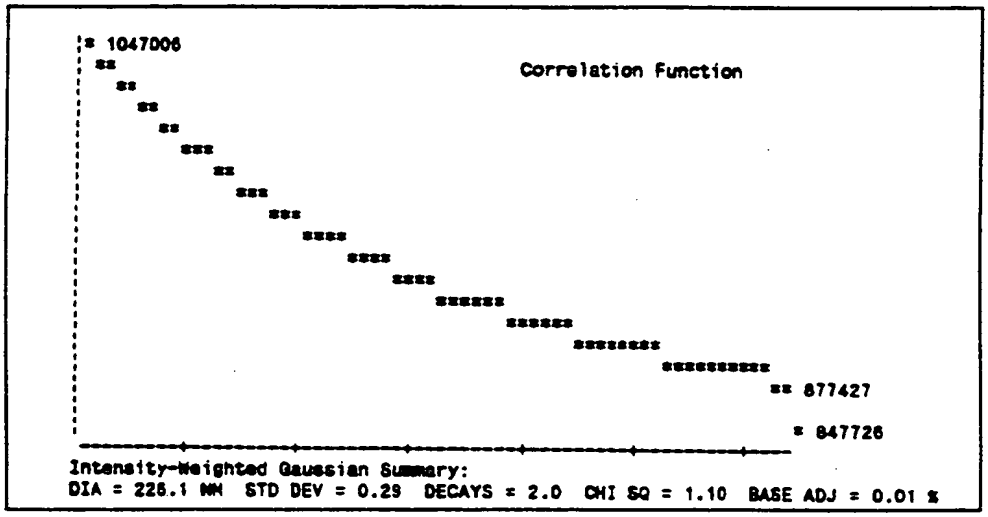

Figure 9a: Autocorrelation function for an IV fat emulsion.

Let us make a visual comparison between Figure 9a and 8a, obtained for the narrow 91 nm latex standard. The shapes of the two decaying curves appear to be quite similar, which is somewhat surprising given the differences between the two samples. Qualitatively, we conclude that the average, or characteristic, particle diameter associated with Figure 9a must be roughly twice that associated with Figure 8a. The reason: both curves possess about the same number of "decays" in falling to the 64th channel, and the channel width for the latter sample is *twice* that of the former.

Exhibit D

Back to the Table of Contents

An Introduction to Statistics - Lesson 6

The Bell-shaped, Normal, Gaussian Distribution

Lesson Overview

The Bell-shaped, Normal, Gaussian Distribution

It can be shown under very general assumptions that the distribution of independent random errors of observation takes on a **normal** distribution as the number of observations becomes large. Although others were involved, Gauss was one of the first to characterize this distribution and hence it is often named after him. It is also shaped like a bell, hence yet another name. The term used in the title above is rather redundant, but serves to emphasize that the three are identical. You can graph this curve on your calculator as seen below by entering the following function: $y=e^{-x^2/2}/\sqrt{(2\pi)}$, where e is the transcendental number 2.71828... and π is the more familiar, but also transcendental number 3.14159.... The π in the formula only serves to **normalize** the total area under the curve. When we normalize something, we make it equal to some **norm** or standard, usually one (1).

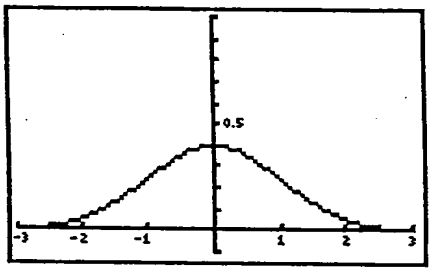

The standard normal distribution

The height of the curve represents the probability of the measurement at that given distance away from the mean. The total area under the curve being one represents the fact that we are 100% certain (probability = 1.00) the measurement is somewhere. Technically, this is the **standard normal** curve which has $\mu=0.0$ and $\sigma=1.0$. Other applications of the normal curve do not have this restriction. For example, intelligence has often been cast, allbeit controversially, as **normally distributed** with $\mu=100.0$ and $\sigma=15.0$. This is represented below. Our function has been modified to $y=e^{-(x-\mu)^2/2\sigma^2}/(\sigma\sqrt{(2\pi)})$

Normally distributed IQs

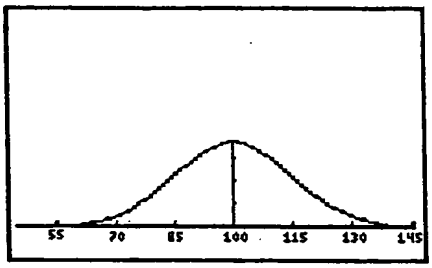

Other things which may take on a normal distribution include body temperature, shoe sizes, diameters of trees, *etc.* It is also important to note the **symmetry** of the normal curve. Some curves may be slightly distorted or truncated beyond certain limits, but still primarily conform to a "heap" or "mound" shape (see below). This is often an important consideration when analyzing data or samples taken from some unknown population.

The Empirical Rule

For a normally distributed data set, the **empirical rule** states that 68% of the data elements are within one standard deviation of the mean, 95% are within two standard deviations, and 99.7% are within three standard deviations. Graphically, this corresponds to the area under the curve as shown below for 1 and 2 standard deviations. The empirical rule is often stated simply as **68-95-99.7**. Note how this ties in with the range rule of thumb, by stating that 95% of the data usually falls within two standard deviations of the mean.

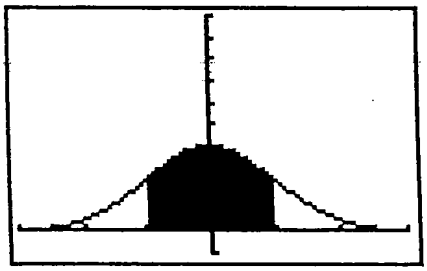

Data within 1σ (left) and 2σ (right)

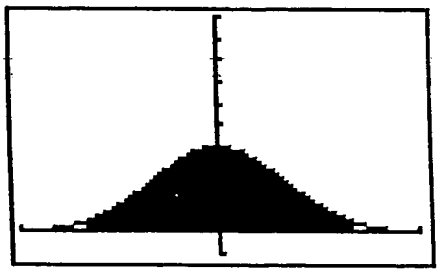

The author usually claims an IQ of at least 145. We can see from the above information that this would put him about three standard deviations above the population mean (100+3•15=145). Hence, if we accept the hypothesis that IQs are normally distributed, 99.85% of the population would have a lower IQ and 0.15% a higher one. Please especially note that if 99.7% of the population is within three standard deviations of the mean, the remaining 0.3% is distributed with half beyond three standard deviations below the mean and the other half beyond three standard deviations above the mean. This is a result of the symmetry (due to the fact that x is squared, it matters not if it is positive or negative) of the curve. In practical terms, in a population of 250,000,000; 249,625,000 would have an IQ lower than 145 and 375,000 would have an IQ higher. Because of the small area of these regions, they are often referred to as **tails**. Depending on the circumstances, we may be interested in **one tail** or **two tails**.

Several societies exist which cater to individuals with high IQs. Some specific examples would be MENSA, Triple Nine, Mega, *etc.*.

Another important charateristic of this distribution is that it is of **infinite extent**. In practical terms, IQs below 0 (6.67σ) or above 210 (7.33σ) (ceiling scores such as Marilyn Vos Savant's are difficult to interpret) do not occur. A recently popularized manufacturing goal has been termed Six Sigma. One

would think this would corresponds with about 3.4 defects per billion, but their web site implies it is 200 per million. A typically good company operates at less than four sigma or 99.997% perfect. This corresponds closer to 32 defects per million. If you have ever purchased a "lemon" (a colloquialism for bad car, perhaps one built on a Monday) you can appreciate such striving for perfection. Other similar examples would be the large increase in errors related to perscription drugs being dispensed or the case of the Florida patient who had the wrong leg amputated.

Chebyshev's Theorem

Chebyshev (1821-1894) was a preeminent Russian mathematician who primarily worked on the theory of prime numbers, although his writings covered a wide range of subjects. One of those subjects was probability and his theorem applies to any data set, not only normally distributed data sets. His theorem states that the portion of any set of data within K standard deviations of the mean is always at least $1-1/K^2$, where K may be any number greater than 1.

For K=2, we see that $1-1/2^2=1-1/4=3/4$, which is 75% of the data must always be within two standard deviations of the mean.

For K=3, we see that $1-1/3^2=1-1/9=8/9$, which is about 89% of the data must always be within three standard deviations of the mean.

If we consider the data set 50, 50, 50, and 100, we will discover that the sample standard deviation (s) is 25, and the upper score falls exactly at $2s$ above the rest. However, since the mean is 62.5, it is well within $2s$. Added 5 more scores of 50 we find the mean is now 55.6 and the standard deviation now 16.7. We see that two standard deviations above the mean now extends to 88.9 and we have one data point outside that, but within three standard deviations. The general concept of being able to find the mean of a data set and determine how much of it is within a certain distance (number of standard deviations) of the mean is an important one which we will continue in the next lesson.

Note: here is an example of a data set with k=2 and only 75% of the data within the proscribed limits. It comes to us from Hogg and Craig (1978, p. 70) in "Introduction to Mathematical Statistics". (5th ed.) via the AP STAT list server on May 31, 2000. Let the discrete random variable x have probabilities 1/8, 6/8, 1/8 at the points x= -1, 0, 1 respectively. μ=0 and σ^2=1/4. If k=2, then $1/k^2$=1/4 and we thus attain the bound given by Chebyshev's inequality.

BACK HOMEWORK ACTIVITY CONTINUE

- e-mail: calkins@andrews.edu
- voice/mail: 269 471-6629/ BCM&S Smith Hall 106; Andrews University; Berrien Springs,
- **classroom:** 269 471-6646; Smith Hall 100/**FAX:** 269 471-3713; MI, 49104-0140
- home: 269 473-2572; 610 N. Main St.; Berrien Springs, MI 49103-1013
- URL: http://www.andrews.edu/~calkins/math/webtexts/stat06.htm

Exhibit E

Large Versus Small Unilamellar Vesicles Mediate Reverse Cholesterol Transport In Vivo Into Two Distinct Hepatic Metabolic Pools

Implications for the Treatment of Atherosclerosis

Wendi V. Rodriguezа, Kirstin D. Mazany, Arnold D. Essenburg, Michael E. Pape, Thomas J. Rea, Charles L. Bisgaier, Kevin Jon Williams

Abstract Phospholipid liposomes are synthetic mediators of "reverse" cholesterol transport from peripheral tissue to liver in vivo and can shrink atherosclerotic lesions in animals. Hepatic disposal of this cholesterol, however, has not been examined. We compared hepatic effects of large (≈120-nm) and small (≈35-nm) unilamellar vesicles (LUVs and SUVs), both of which mediate reverse cholesterol transport in vivo but were previously shown to be targeted to different cell types within the liver. On days 1, 3, and 5, rabbits were intravenously injected with 300 mg phosphatidylcholine (LUVs or SUVs) per kilogram body weight or with the equivalent volume of saline. After each injection, LUV- and SUV-injected animals showed large increases in plasma concentrations of unesterified cholesterol, indicating mobilization of tissue stores. After hepatic uptake of this cholesterol, however, SUV-treated animals developed persistently elevated plasma LDL concentrations, which by day 6 had increased to more than four times the values in saline-treated controls. In contrast, LUV-treated animals showed normal LDL levels. By RNase protection assay, SUVs suppressed hepatic LDL receptor mRNA at day 6 (to 61±4% of control, mean±SEM), whereas LUVs caused a statistically insignificant stimulation. Hepatic HMG-CoA reductase message was also significantly suppressed with SUV, but not LUV treatment, and hepatic 7α-hydroxylase message showed a similar trend. These data on hepatic mRNA levels indicate that SUVs, but not LUVs, substantially perturbed liver cholesterol homeostasis. We conclude that LUVs and SUVs mobilize peripheral tissue cholesterol and deliver it to the liver, but to distinct metabolic pools that exert different regulatory effects. The effects of one of these artificial particles, SUVs, suggest that reverse cholesterol transport may not always be benign. In contrast, LUVs may be a suitable therapeutic agent, because they mobilize peripheral cholesterol to the liver without suppressing hepatic LDL receptor mRNA and without provoking a subsequent rise in plasma LDL levels. (*Arterioscler Thromb Vasc Biol.* 1997;17:2132-2139.)

Key Words • atherosclerosis • HDL • gene expression • cholesterol • therapy

Four decades ago, the intravenous administration of aqueous dispersions of PL was shown to cause rapid, substantial shrinkage of lipid-rich arterial lesions in animals.[1] This striking finding has since been confirmed in a variety of experimental models of atherosclerosis (reviewed in Reference 2). Subsequent mechanistic studies indicated that dispersed PLs self-assemble into concentric spherical bilayers known as liposomes or vesicles.[3] Furthermore, when intravenously injected at sufficient doses, initially cholesterol-free PL vesicles remain intact in the bloodstream and are capable of extracting cholesterol from both lipoproteins and peripheral tissues.[2,4] Thus, these circulating particles act as a sink for cholesterol, which is shuttled to them from tissues by HDL and other small acceptors of cholesterol.[2,4-7] Because the liver serves as the predominant organ for the clearance of PL vesicles, it has been suggested that the antiatherogenic effects of these particles result from their ability to act as synthetic mediators of RCT from peripheral tissues to the liver.[2,5]

Hepatic disposal of cholesterol transported from the periphery to the liver, however, is not well understood. Radioisotopic studies have suggested that cholesterol of HDL, the apparent natural mediator of RCT,[8] is efficiently converted into bile acids by the liver and then excreted.[9-12] In contrast, direct measurements of sterol mass showed that accelerated delivery of cholesterol to the liver in vivo by apoE-rich HDL produces no change in biliary output of cholesterol or bile acids, but instead stimulates hepatic acyl-CoA:cholesterol acyltransferase and enhances VLDL secretion.[13] Similar results, including LDL receptor suppression, have been reported in other situations involving cholesterol enrichment of hepatic cells.[14-17] Moreover, intravenous infusion of apoA-I/PL disks into humans to enhance RCT causes a sustained rise in plasma levels of LDL.[18] Taken together, these effects are more consistent with events leading to

Received February 29, 1996; revision accepted December 18, 1996.

From the Department of Biochemistry, Medical College of Pennsylvania, Philadelphia, Pa (W.V.R., K.J.W.); and Vascular and Cardiac Diseases, Parke-Davis Pharmaceutical Research, Division of Warner-Lambert Co, Ann Arbor, Mich (K.D.M., A.D.E., M.E.P., T.J.R., C.L.B.). Dr Williams is now with the Division of Endocrinology, Jefferson Medical College of Thomas Jefferson University, Philadelphia, Pa.

Presented in part at the 68th Scientific Sessions of the American Heart Association, Anaheim, Calif, November 13-16, 1995, and published in abstract form (*Circulation*. 1995;92[suppl I]:I-556).

Correspondence to Kevin Jon Williams, Division of Endocrinology, Thomas Jefferson University, 1020 Locust St, Suite 349, Philadelphia, PA 19107-6799 E-mail kevin.jon.williams@mail.tju.edu or Charles L. Bisgaier, Vascular and Cardiac Diseases, Parke-Davis Pharmaceutical Research, 2800 Plymouth Rd, Ann Arbor, MI 48105 E-mail bisgaic@aa.wl.com.

Selected Abbreviations and Acronyms

apo = apolipoprotein
AU = arbitrary units
CE = cholesteryl ester
CETP = CE transfer protein
EC = esterified cholesterol
LUV = large unilamellar vesicle
MLV = multilamellar vesicle
PL = phospholipid
RCT = reverse cholesterol transport
SUV = small unilamellar vesicle
TC = total cholesterol
UC = unesterified cholesterol

the promotion, not the inhibition, of atherogenesis. Thus, depending on hepatic responses, not all agents that enhance RCT will be unambiguously beneficial.

In this study, we sought to determine the effect of liposomal structure on hepatic responses to enhanced RCT mediated by these synthetic particles. We compared LUVs (~120-nm), which have been shown to be catabolized in the liver primarily by Kupffer cells,[19] versus SUVs (~35-nm), which are directed mainly to parenchymal cells.[20] Prior work has shown that both LUVs and SUVs mobilize cholesterol from lipoproteins and peripheral tissues, thereby enhancing RCT in vivo.[6] The response of the liver to repeated injections of these two liposomal preparations over several days was determined by monitoring the concentrations of major plasma lipopr tein species and by measuring mRNA levels of key hepatic enzymes and proteins responsible for maintaining hepatic cholesterol homeostasis.

Methods

Materials

Egg phosphatidylcholine (>95% pure, Coatsome NC-10S) was purchased from Princeton Lipids. Human HDL$_2$ was isolated from fresh plasma by sequential ultracentrifugation ($1.12<d<1.21$ g/mL).[21] All other chemicals and solvents were of analytical grade and purchased from Fisher Scientific Co.

Preparation of Vesicles

Three days before the start of the experiment in vivo, LUVs and SUVs were prepared at a concentration of 100 mg/mL. Six 6-g portions of solid egg phosphatidylcholine were each placed into 50-mL conical polypropylene centrifuge tubes, hydrated with 30 mL of filter-sterilized 150 mmol/L NaCl, 20 mmol/L HEPES, pH 7.4 (HEPES-buffered saline), and vortexed to generate MLVs. These preparations were kept overnight at 4°C. To generate LUVs, the MLVs were extruded 10 times under medium pressures (250 to 300 psi) through two stacked polycarbonate filters (100-nm pore size) that had been fitted into a 10-mL water-jacketed thermobarrel Extruder (Lipex Biomembranes). To generate SUVs, 30-mL batches of MLVs were each subjected to three 20-minute cycles of sonication in 50-mL round-bottom Pyrex glass tubes at 0°C under nitrogen (power setting=3, duty cycle=50%, Branson stud tip sonifier, VWR Co). The initially milky suspension clarified during this procedure. After sonication, batches were then centrifuged at 20 000*g* for 30 minutes to remove titanium shed from the probe during sonication.

The two vesicle preparations, LUVs and SUVs, were sterilized by passage through 0.45-μm Nalgene bottle-top filters, assayed for PL concentrations,[22] and diluted with sterile HEPES-buffered saline to 100 mg PL per milliliter before injection. Consistent with prior literature, the diameters of the LUVs and SUVs generated were found to be 123±35 and 34±30 nm (mean±SD), respectively, determined by quasi-elastic light scattering using a Nicomp model 370 submicron laser particle sizer, equipped with a 5-mW He-Ne laser (Pacific Scientific).[6]

Experimental Design In Vivo

Normal 3- to 4-kg female New Zealand White rabbits (Hazelton Farms, Denver, Pa) were randomly distributed into three groups (n=4, LUV or saline treatment; n=3, SUV treatment). Approximately 3 mL of blood was collected from each animal via a medial auricular artery every morning during the study. Blood samples were immediately mixed with EDTA for anticoagulation (final concentration, 2 mmol/L in blood) and *N*-ethylmaleimide to inhibit lecithin:cholesterol acyltransferase (final concentration, 5 mmol/L).

On days 1, 3, and 5, right after the morning's blood collection, LUVs or SUVs (300 mg of PL per kilogram body weight), or the equivalent volume of HEPES-buffered saline, were bolus-injected into a marginal ear vein of each animal (approximately 10 mL per injection, infused over ~30 seconds). Immediately after blood collection on day 6, all animals were killed (100 mg pentobarbitol per kilogram IV),[23] and several 100- to 200-mg liver samples were collected from each animal and snap-frozen in liquid nitrogen. Tissue samples were stored at −70°C until isolation of total RNA and lipid analysis.

Analyses of Plasma and Plasma Fractions

Triglyceride concentrations in whole plasma were determined by using a commercially available kit (Triglyceride G, Wako Chemicals USA, Inc). Whole-plasma concentrations of TC (equal to unesterified and esterified forms) and UC concentrations in whole plasma were directly determined enzymatically,[24] and EC was calculated by difference. Agarose gel electrophoresis of whole plasma followed by lipid staining with Sudan black[4,25] and rocket immunoelectrophoresis to quantitate whole-plasma rabbit apoB, reported in AU,[17,26] were performed as previously described. Preliminary studies indicated that these rocket assays, which are performed in detergent,[26] are not affected by the presence of liposomes. Size distributions of plasma particles carrying TC and UC were determined by Superose 6HR high-performance gel chromatography (Rainin Instrument Co, Inc), including an on-line post-column analyzer, as previously described.[27,28] Areas under the peaks were used to calculate the percent distribution of TC and UC corresponding to VLDL, LDL, and HDL size ranges in the elution profiles (Dynamax and Compare Module Software, Rainin Instrument Co, Inc, developed for Macintosh computers). Next, the absolute concentrations of TC and UC in each lipoprotein size range were determined by multiplying these percent distribution values by the independently determined TC and UC values in whole plasma. Absolute EC values in each lipoprotein fraction were determined by the difference between the calculated TC and UC in each lipoprotein fraction. Plots of the distributions of absolute lipid content by particle size were prepared similarly, ie, the total area under each TC and UC elution curve from the on-line post-column analyzer was normalized to the corresponding whole-plasma assay result. Absolute EC distribution curves were then determined by difference.

Analytical Methods for Determination of Hepatic Lipids

Hepatic phosphatidylcholine, phosphatidylethanolamine, CE, UC, and triglyceride were extracted in the presence of 4-hydroxycholesterol internal standard, separated by silica column high-performance liquid chromatography, and then quantitated by an evaporative light-scattering detector, as previously described.[28] Notice that these tissue CE determinations include the mass of both the steryl and fatty acyl moieties, whereas the EC measurements in plasma and plasma fractions include only steryl mass.

Hepatic mRNA Analysis

Rabbit cDNAs encoding the LDL receptor, HMG-CoA reductase, 7α-hydroxylase, and CETP were prepared in polymerase chain reactions using primers based on phylogenetically conserved sequences and then cloned into the pBluescript II SK (+) plasmid (Stratagene Cloning Systems). The identity of each cloned cDNA was confirmed by sequencing, as described in detail by Rea et al.[29] For each cloned cDNA, an unlabeled sense mRNA product, to be used as an internal standard, and a labeled antisense mRNA probe were synthesized. Both synthetic mRNAs were designed to contain the partial coding sequence from rabbit, linked to a short sequence from the plasmid.

Total RNA was isolated from the snap-frozen rabbit liver samples using RNAzol (Cinna/Biotecx Inc), quantified by A_{260}, and assessed for degradation by agarose electrophoresis. Messenger RNAs of interest were quantified by an internal standard/RNase protection assay, as described previously in detail.[30] Each protection assay contained (1) 30 μg of total liver RNA, (2) the synthetic unlabeled sense mRNA internal standard (30 pg LDL receptor, 10 pg HMG-CoA reductase, 10 pg 7α-hydroxylase, or 5 pg CETP), and (3) 1.0 ng of the synthetic radiolabeled antisense mRNA probe (specific activity, 2×10^8 cpm/μg). After digestion with RNase, protected mRNA probes were quantified by polyacrylamide gel electrophoresis and then autoradiography using a PhosphorImager (Molecular Dynamics). Probes protected by authentic versus internal-standard mRNA differed in molecular weight by the size of the incorporated plasmid sequence and were directly identified by control reactions in which either rabbit liver RNA or the unlabeled internal standard mRNA was individually omitted. The ratio of radioactivity in the two protected bands, multiplied by the known amount of internal-standard mRNA and corrected for molecular weight differences between authentic and internal-standard mRNA, gave the mass of hepatic liver mRNA of interest.

Protein Uptake by Large and Small PL Vesicles In Vitro

To determine whether there are systematic differences in the acquisition of proteins by LUVs versus SUVs, these particles were incubated in vitro for 4 hours at 37°C with HDL_3, using a PL ratio of 5:1 (vesicle:HDL), which is similar to ratios achieved in vivo and does not disrupt vesicle structure.[31] PL vesicles were then separated from the HDL by passage over a 130×1.5-cm column of Sepharose CL-6B. Purity of these modified liposomes was verified by the absence of detectable esterified cholesterol[24] by gas-liquid chromatography.[32,33] The modified LUVs and SUVs were analyzed for protein content by modified Lowry,[34] PL content enzymatically,[35] and protein species by SDS–polyacrylamide gel electrophoresis.

Statistical Analyses

ANOVA was used to compare the three experimental groups. When ANOVA indicated differences among the groups, pairwise comparisons between groups were performed using the Student-Neumann-Keuls q statistic.[36] Unless otherwise indicated, all results are displayed as mean±SEM, (n=4, LUV and saline groups; n=3, SUV group). Absent error bars in figures indicate SE values smaller than the drawn symbols.

Results

Alterations in Plasma Lipids and Lipoproteins in Response to Repeated Injections of PL Vesicles

Three intravenous injections of PL into normal rabbits caused large increases in the plasma concentrations of UC, indicating mobilization of tissue stores (Fig 1A), similar to previous findings.[1,2,4,5,37] LUVs had a larger effect than SUVs on plasma UC concentrations, consistent with the prior observation that per milligram of administered PL, LUVs mobilize cholesterol more efficiently.[6] SUVs caused a rise in plasma concentrations of EC, confirming prior reports of this effect after hepatic uptake of cholesterol mobilized by these particles.[4,5] Surprisingly, although LUVs mobilize more cholesterol to the liver, there was no effect at all on plasma EC concentrations (Fig 1B).

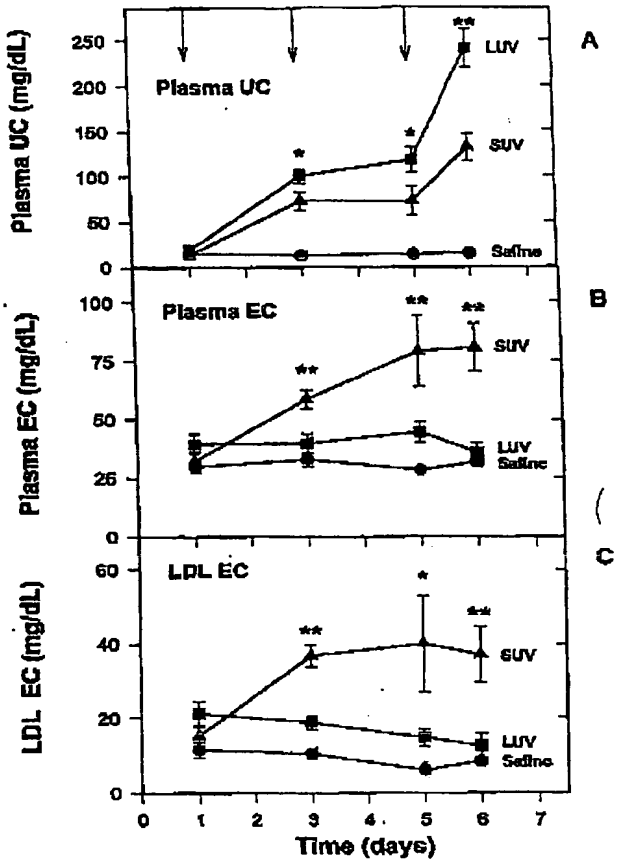

Fig 1. Plasma unesterified cholesterol (A), plasma esterified cholesterol (B), and LDL esterified cholesterol concentrations (C) in New Zealand White rabbits after repeated injections of LUVs (■) or SUVs (▲) at a dose of 300 mg/kg, or the equivalent volume of saline (●). Arrows indicate intravenous injections of PL vesicles or saline on days 1, 3, and 5. Plasma samples on those days were obtained immediately before the injections. Each data point displays the mean±SEM. In B and C, LUV values were statistically indistinguishable from the corresponding control (saline) values, except for C, day 3 ($.01<P<.05$). In all three panels, SUV values after day 1 were greater than control ($P<.01$). *$P<.05$, **$P<.01$; significant differences between LUV and SUV values.

Because EC cannot be transported to any great extent by PL vesicles owing to their lack of a hydrophobic core, we sought to determine which lipoprotein carried the extra plasma EC after SUV injection. Gel filtration revealed that most of the increase in whole-plasma EC was transported by LDL-sized particles (Fig 1C, Table 1, and Fig 2A). Under these conditions, liposomal remnants would not appear in this size rang , because

TABLE 1. Unesterified and Esterified Cholesterol Concentrations in Wh le Plasma and in VLDL-, LDL-, and HDL-Sized Particl s on Day 6

	Whole Plasma		VLDL		LDL		HDL	
Treatment	UC	EC	UC	EC	UC	EC	UC	EC
LUV	239.9±20.6*	36.1±4.1	207.0±20.7*	2.0±1.9	21.9±0.7*	12.6±3.3	11.0±0.5	21.8±1.4
SUV	131.4±14.7*	80.7±10.3*	51.4±4.4†	6.3±1.9	61.1±9.1*	37.1±7.5*	19.0±1.2*	37.3±2.1*
Saline	15.3±0.8	31.8±2.0	0.9±0.2	0.5±0.1	4.2±0.4	8.4±0.7	10.2±0.6	23.0±1.7

All values are mean±SEM expressed as milligrams lipid per deciliter plasma. Each LUV value was significantly different from the corresponding SUV value ($P<.01$), except for VLDL EC (not significant).
*$P<.01$; †$P<.05$; significantly different from saline control.

vesicle structure is stable in plasma at 300 mg/kg[4,5,21] and remnants that form at lower vesicle doses are exclusively PL-apoprotein disks that coelute with HDL.[31,36] Quantitatively, SUVs increased plasma concentrations of LDL EC to over fourfold compared with saline control (Table 1), whereas injections of LUVs caused a small but statistically insignificant decrease during the study (Fig 1). Rabbit apoB assays of plasma from day 6 showed a trend toward higher values in the SUV group (0.31±0.04 AU) than the LUV group (0.16±0.07 AU). These results suggest a proportionately greater increase in LDL EC than in plasma apoB after SUV administration, raising the possibility of increased LDL size, which was confirmed by a slight shift on the EC elution profile (Fig 2A, EC profile after SUV treatment). No shifts were evident in any HDL EC peaks (Fig 2A). The SUV-mediated increase in LDL concentration was confirmed by agarose gel electrophoresis followed by Sudan black staining,[25] which revealed a darker but otherwise unremarkable β-band (Fig 2B). As previously reported,[4] the SUVs in plasma exhibited a mobility ahead of LDL owing to their acquisition of plasma proteins, chiefly from HDL. In contrast, plasma LUVs exhibited essentially the same mobility as freshly prepared, protein-free vesicles, ie, just above the origin (Fig 2B; discussion to follow).

Fractionation data for all particle sizes from the final bleed on day 6 are summarized in Table 1. Notice that the additional UC mobilized into the plasma of LUV-treated animals was mainly confined to the VLDL size range, while the additional UC in the SUV-treated animals was in both the VLDL and LDL size ranges, consistent with the smaller size but greater heterogeneity of SUVs compared with LUVs (see "Methods"). Also, lipoprotein fractionation revealed an increase in the concentration of HDL EC in SUV-treated animals. This increase in HDL EC, however, represented only a small fraction of the total cholesterol mass mobilized by the injected vesicles. No significant changes in plasma concentrations of triglycerides were observed (data not shown), consistent with prior studies.[37]

Alterations in Hepatic Lipids and mRNA in Response to Repeated Injections of PL Vesicles

On day 6, 24 hours after the third injection, hepatic samples were taken for lipid and mRNA analyses. Because vesicles in the bloodstream eventually achieve a molar ratio of UC:PL of about 0.8,[6] which is far higher than the ratio of 0.12 found in normal hepatic tissue (Table 2), we anticipated that hepatic uptake of vesicles might increase this ratio in liver. Both types of PL vesicles did substantially increase the hepatic UC:PL ratio (Table 2; $P<.01$), consistent with liposomal delivery of cholesterol mass to the liver. With both types of particles, the significant increase in the hepatic UC:PL ratio appeared to result from increased hepatic UC and decreased hepatic PL, although only the SUV-induced decrease in hepatic PL reached statistical significance compared with saline control. No effects on hepatic triglyceride content were observed (data not shown).

Hepatic mRNA levels for key enzymes in cholesterol homeostasis are shown in Fig 3. The three injections of SUVs caused ≈40% to 50% suppression of hepatic mRNA levels for the LDL receptor and HMG-CoA reductase. A similar though statistically insignificant trend was seen with 7αa-hydroxylase. These results are consistent with regulatory effects seen after substantial cholesterol loading of parenchymal cells, which compensate by suppressing their uptake of LDL and their synthesis of sterol (see References 15, 17, 39, and 40). In contrast, the three injections of LUVs caused increases, though statistically insignificant, in each of these messages. Finally, LUVs, but not SUVs, significantly suppressed hepatic mRNA for CETP.

Protein Uptake by Large and Small PL Vesicles In Vitro

Based on the electrophoretic mobilities in Fig 2B, we sought to quantitate the acquisition of proteins by LUVs versus SUVs. After incubation with HDL, LUVs acquired 1.09 μg of protein per milligram of liposomal PL, whereas SUVs acquired 40.4 μg/mg, ie, almost 40 times as much. Consistent with prior literature,[4,41] SDS–polyacrylamide gel electrophoresis confirmed that the major protein acquired by both LUVs and SUVs was apoA-I (data not shown).

Discussion

In the current study, we have demonstrated that the metabolic effects from several days of enhanced RCT in vivo strongly depend on the particle that carries cholesterol from the periphery to the liver. Furthermore, RCT mediated by some particles, such as SUVs (see "Results") and HDL-like complexes (see References 13 and 18), can produce metabolic consequences that may not be benign.

Our results with SUVs are entirely consistent with prior literature concerning cholesterol enrichment of hepatocytes. When liver cells were cholesterol enriched in vivo by a single injection of apoE-rich HDL that was rapidly cleared from plasma into liver[13] or by feeding nonhuman primates long term on atherogenic diets,[39] similar results were observed, including LDL receptor suppression and lipoprotein oversecretion. Similarly, cholesterol enrichment of hepatocytes in vitro causes suppression of LDL receptors[42,43] and HMG-CoA re-

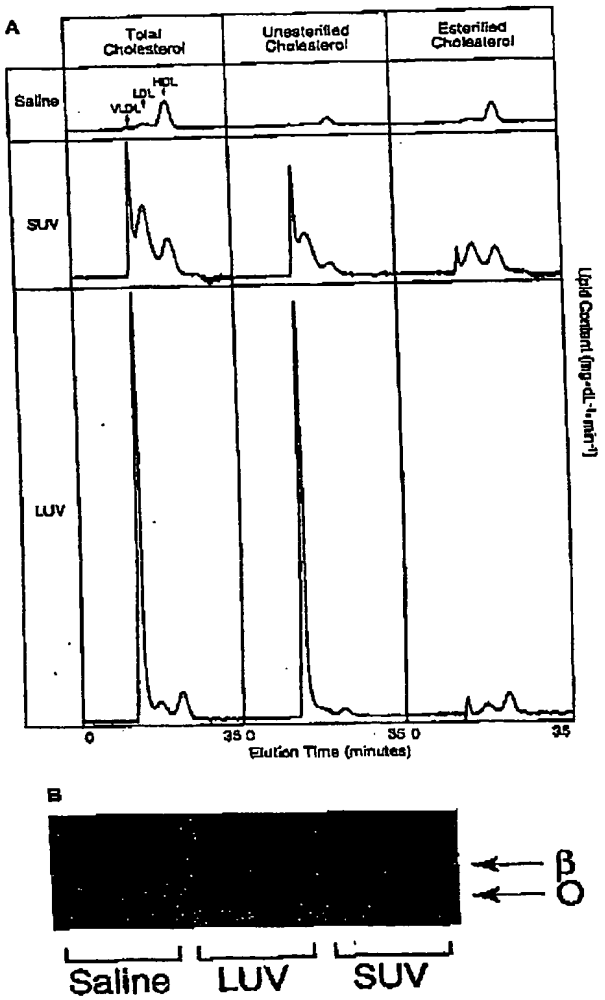

FIG 2. Fractionations of plasma from day 6 after repeated injections of LUVs, SUVs, or saline. A, Distributions of lipids in whole plasma by particle size. Plasma samples were gel filtered through a Superose 6HR column, and eluents were assayed for TC and UC. The total area under each curve was normalized to the whole-plasma assay for TC or UC. The EC curve was generated by difference. Plots from one animal in each group are shown, with all panels drawn to the same scale. Specific lipoproteins are identified in the upper left-hand plot. The area under the LDL EC peaks in the saline, SUV, and LUV animal were the same, much larger, and slightly smaller, respectively, than on day 1. B, Distributions of plasma lipids by particle charge. Four-microliter plasma samples from two animals in each group at day 6 were electrophoresed through 0.5% agarose and then stained with Sudan black. O indicates origin and β, migration of an LDL standard.

TABLE 2. Lipid Content in Livers of Animals on Day 6 of Treatm nt With LUVs, SUVs, or Saline

Treatment	UC	CE	PL	UC:PL Ratio (mol/mol)
LUV	5.3±0.2	1.6±0.8	65.0±1.6*	0.16±0.01†
SUV	4.6±0.5	2.6±1.1	53.1±3.0†	0.16±0.02†
Saline	4.3±0.2	2.9±1.2	68.3±1.5	0.12±0.01

Mass values are shown as mean±SEM, expressed as microgram lipid per milligram protein in liver (n=4 animals per treatment group). Phospholipid content equals phosphatidylcholine plus phosphatidylethanolamine.
*$P<.01$; significant differences between LUV and SUV values.
†‡$P<.01$; significantly different from saline control.

LDL receptor, were suppressed, and consequently, plasma LDL concentrations rose. It is nonetheless surprising that the metabolic effects on the liver of RCT mediated by SUVs in the current study or by apoE-rich

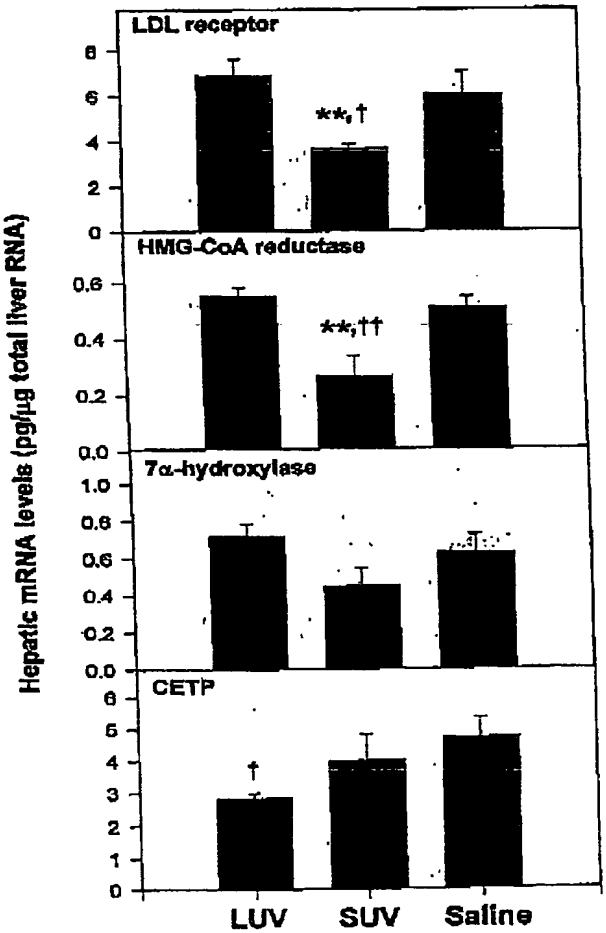

FIG 3. Hepatic mRNA levels for the LDL receptor, HMG-CoA reductase, 7α-hydroxylase, and CETP, expressed as picograms of specific mRNA per microgram total liver mRNA. Messages in liver samples obtained at day 6 were quantified by RNase protection assay. Each data point displays the mean±SEM. *$P<.05$, **$P<.01$; significant differences between LUV and SUV values. †$P<.05$, ††$P<.01$; significantly different from saline control.

ductase,[44-47] as well as enhancement of apoB secretion.[16,43,48,49] The expression of hepatic 7α-hydroxylase is stimulated by cellular cholesterol enrichment in rats[50] but inhibited in rabbits,[17,40] consistent with the trend in Fig 3. Thus, RCT by these synthetic SUVs was associated with events that are entirely consistent with known molecular consequences of cellular cholesterol enrichment: sterol-responsive messages in the liver, such as the

particles in a previous study[13] appear to be inconsistent with antiatherogenic actions.

Our results with LUVs, however, were starkly different. Prior work has shown that LUVs transport significantly more peripheral cholesterol in vivo to the liver than do SUVs,[6] and yet there was no suppression of sterol-responsive messages in the liver and no rise in plasma LDL concentrations (Figs 1 through 3). We propose three possible explanations for the difference in metabolic response to LUVs versus SUVs. First, it has been reported that LUVs are taken up by Kupffer cells,[19] whereas SUVs are primarily directed toward hepatic parenchymal cells.[20] Presumably, this is partly a mechanical consequence of hepatic architecture: hepatic endothelial fenestrae are oval openings of about 100×115 nm,[51,52] through which SUVs of 35-nm diameter can readily pass and gain access to parenchymal cells. LUVs of 120-nm diameter or slightly larger will not pass easily and are cleared instead by the macrophage Kupffer cells that line liver sinusoids. While SUVs also have access to Kupffer cells, their sheer number (~10 times as many SUVs as LUVs per milligram of PL) appears to saturate the reticuloendothelial system, and so parenchymal cells predominate in their clearance (see Reference 20).

Cholesterol-clearance pathways mediated by parenchymal versus Kupffer cells are likely to have distinct metabolic consequences. Direct delivery of cholesterol to parenchymal cells by SUVs would be expected to suppress sterol-responsive messages. Delivery of cholesterol to Kupffer cells can be followed by gradual transfer of lipid to parenchymal cells,[19,53] for example, via the extensions of Kupffer cells that reach down through the space of Disse to make physical contact with parenchymal cells.[53] The rate of sterol delivery to the parenchymal cells by transfer from Kupffer cells can be slower than by direct uptake; the chemical form of the sterol may be altered by the Kupffer cells before transfer (see Reference 54); and, on the basis of other pathways for lipid transfer among liver cells,[54a] the process of transfer from Kupffer to parenchymal cells may be regulated, whereas SUV clearance does not appear to be.[5,20]

The second possible explanation for the difference in metabolic response to LUVs versus SUVs is based solely on differences in the kinetics of their delivery of cholesterol to the liver. In mice, LUVs are cleared from plasma somewhat more slowly than are SUVs and thereby produce a relatively constant delivery of cholesterol mass to the liver from the time of injection until the bulk of injected material is cleared.[6] Similarly, in rabbits, LUVs are cleared with a $t_{1/2}$ of ~27 hours (W.V. Rodrigueza, M.J. Hope, unpublished studies, 1997), whereas SUVs are cleared more rapidly,[5] thereby delivering a large bolus of cholesterol mass to the liver between 4 and 12 hours after injection, which is followed by a rise in plasma EC concentration.[5] The slow, steady delivery by LUVs may avoid disrupting hepatic cholesterol homeostasis, while the more rapid uptake of SUV cholesterol may overwhelm the ability of the liver to maintain homeostasis, thereby provoking suppression of hepatic LDL receptors (see Reference 15).

The third possible explanation is based on the striking quantitative difference in protein adsorption between the two types of vesicles (Fig 2B and "Results"), which is presumably a result of their distinct surface curvatures.[55] Thus, it is conceivable that SUVs, but not LUVs, would avidly strip apoE from VLDL, thereby slowing its clearance from plasma and favoring its conversion to LDL (see Reference 56). This scenario, however, would not explain the divergent effects of the two types of vesicles on hepatic gen expression (Fig 3). Alternatively, differences in adsorbed apoproteins might play a role in directing the PL vesicles into different hepatic metabolic pools, although there is no direct evidence that apoproteins mediate hepatic uptake of these particles.[5,57]

Our results with hepatic CETP message were unexpected; namely, suppression by LUV injections and no significant effect of SUV injections, despite cholesterol delivery. Notice that CETP mRNA differs from the other three messages that we studied: it is equally distributed between hepatic parenchymal and nonparenchymal cells on a per-gram basis, whereas hepatic mRNAs for the LDL receptor, HMG-CoA reductase, and 7α-hydroxylase are >90% in parenchymal cells.[29] Prior reports indicate that hyperlipidemia in rabbits is associated with increases in plasma CETP mass and hepatic message,[58] although separate effects on parenchymal and nonparenchymal cells are not known. Also, suppression of CETP is usually followed by increases in HDL EC,[59] which we did not see here after LUV injections. Our results may not be directly comparable to the study by Quinet et al,[58] however, because we investigated the redistribution of endogenous cholesterol among tissues by artificial particles, whereas the prior work in animals involved enhanced dietary intake. Thus, it is likely that LUVs suppressed hepatic CETP mRNA by depleting cholesterol from a regulatory pool that ordinarily stimulates CETP production and then disposed of this cholesterol into a nonstimulatory pool. SUVs, which are cleared differently, produced no overall effect on CETP message. Because the role of CETP in provoking or preventing atherosclerosis is controversial,[60-62] the importance in atherogenesis of our finding that CETP mRNA is suppressed after LUV injections is not clear. Nevertheless, because LUVs and SUVs produced different effects on CETP mRNA, as well as on the other messages, there is a consistent pattern of divergent regulatory effects between these two synthetic mediators of RCT.

For many reasons, the safe enhancement of RCT is an important medical goal. First, it has been recently accepted that most human heart attacks are caused by rupture-prone lesions that are rich in lipid and foam cell macrophages.[63,64] One goal for treatment of preestablished disease is to stabilize these lesions. Apparently, these lesions can be gradually rendered less dangerous by aggressive lipid-lowering therapy,[65] which presumably reduces lesional content of lipid[65] and possibly tissue factor.[66] We speculate that massive enhancement of cholesterol transport from peripheral tissues to the liver by LUVs in vivo should achieve the same beneficial result quickly and directly. Second, enrichment of vessel wall cells with cholesterol or oxidized derivatives is known to produce substantial dysfunction.[66-69] Cholesterol-enriched endothelial cells lose their ability to produce endothelial-derived relaxing factor,[70,71] and cholesterol-enriched smooth muscle cells exhibit supranormal levels of cytosolic calcium[72] and enhanced proliferation.[73] Many of these effects can be quickly reversed in vitro by removal of the excess cellular UC.[74] We speculate that enhanced RCT should accomplish the same in

vivo, with rapid therapeutic benefit. Third, platelet hyperreactivity can be caused by an increased platelet membrane ratio of UC:PL, which has been described in som human hyperlipidemias.[75-78] Again, a massive enhancement of RCT might produce a rapid therapeutic benefit in this situation by reducing platelet reactivity in vivo.

Ov rall, our findings indicate that these synthetic particles, LUVs and SUVs, mediate RCT in vivo, though with markedly different regulatory effects on the liver. LUVs appear to be the better therapeutic agent, because they mobilize cholesterol from the periphery to the liver without suppressing hepatic LDL receptor message and without provoking a rise in plasma LDL concentrations.

Acknowledgments

W.V. Rodrigueza was an International Research Fellow of the American Heart Association and then supported by a Research Fellowship from the Heart and Stroke Foundation of BC and Yukon, Canada. K.J. Williams is an Established Investigator of the American Heart Association/Genentech. We wish to thank Dr Reynold Homan for assistance with hepatic lipid analyses and Dr Michael C. Phillips for very helpful discussion and suggestions.

References

1. Friedman M, Byers SO, Rosenman RH. Resolution of aortic atherosclerotic infiltration in the rabbit by phosphatide infusion. *Proc Soc Exp Biol Med*. 1957;95:586-588.
2. Williams KJ, Werth VP, Wolff JA. Intravenously administered lecithin liposomes: a synthetic antiatherogenic lipid particle. *Perspect Biol Med*. 1984;27:417-431.
3. Bangham AD, Standish MM, Watkins JC. Diffusion of univalent ions across the lamellae of swollen phospholipids. *J Mol Biol*. 1965; 13:238-252.
4. Williams KJ, Scanu AM. Uptake of endogenous cholesterol by a synthetic lipoprotein. *Biochim Biophys Acta*. 1986;875:183-194.
5. Williams KJ, Vallabhajosula S, Rahman IU, Donnelly TM, Parker TS, Weinrauch M, Goldsmith SJ. Low density lipoprotein receptor-independent hepatic uptake of a synthetic, cholesterol-scavenging lipoprotein: implications for the treatment of receptor-deficient atherosclerosis. *Proc Natl Acad Sci U S A*. 1988;85:242-246.
6. Rodrigueza WV, Pritchard PH, Hope MJ. The influence of size and composition on the cholesterol mobilizing properties of liposomes in vivo. *Biochim Biophys Acta*. 1993;1153:9-19.
7. Rodrigueza WV, Williams KJ, Rothblat GH, Phillips MC. Remodeling and shuttling: mechanisms for synergistic effects between different acceptor particles in the mobilization of cellular cholesterol. *Arterioscler Thromb Vasc Biol*. 1997;17:383-393.
8. Glomset JA. The plasma lecithin:cholesterol acyltransferase reaction. *J Lipid Res*. 1968;9:155-167.
9. Schwartz CC, Halloran LG, Vlahcevic ZR, Gregory DH, Swell L. Preferential utilization of free cholesterol from high-density lipoproteins for biliary cholesterol secretion in man. *Science*. 1978; 200:62-64.
10. Miller LK, Tiell ML, Paul I, Spaet TH, Rosenfeld RS. Side-chain oxidation of lipoprotein-bound [24,25-^{3}H]cholesterol in the rat: comparison of HDL and LDL and implications for bile acid synthesis. *J Lipid Res*. 1982;23:335-344.
11. Esnault-Dupuy C, Chanussot F, Lafont H, Chabert C, Hauton J. The relationship between HDL-, LDL-, liposome-free cholesterol, biliary cholesterol and bile salts in the rat. *Biochimie*. 1987;69:45-52.
12. Pieters MN, Schouten D, Bakkeren HF, Esbach B, Brouwer A, Knook DL, Van Berkel TJ. Selective uptake of cholesteryl esters from apolipoprotein-E-free high-density lipoproteins by rat parenchymal cells in vivo is efficiently coupled to bile acid synthesis. *Biochem J*. 1991;280:359-365.
13. Stone BG, Schreiber D, Alleman LD, Ho CY. Hepatic metabolism and secretion of a cholesterol-enriched lipoprotein fraction. *J Lipid Res*. 1987;28:162-172.
14. Franklin F, Watkins J, Clowes A, Breslow J. Serum lipids and regulation of liver cholesterol synthesis during total parenteral nutrition. *Circulation*. 1976;54:165. Abstract.
15. Spady DK, Turley SD, Dietschy JM. Rates of low density lipoprotein uptake and cholesterol synthesis are regulated independently in the liver. *J Lipid Res*. 1985;26:465-472.
16. Williams KJ, Brocia RW, Fisher EA. The unstirred water layer as a site of control of apolipoprotein B secretion. *J Biol Chem*. 1990; 265:16741-16744.
17. Krause BR, Pape ME, Kieft K, Auerbach B, Bisgaier CL, Homan R, Newton RS. ACAT inhibition decreases LDL cholesterol in rabbits fed a cholesterol-free diet: marked changes in LDL cholesterol without changes in LDL receptor mRNA abundance. *Arterioscler Thromb*. 1994;14:598-604.
18. Kuivenhoven JA, Demacker PNM, Stalenhoef AFH, Pajkrt D, van Deventer SJH, Doran JE, Pritchard PH, Kastelein JJP. Infusion of reconstituted HDL: reverse cholesterol transport in hereditary HDL deficiencies. *Circulation*. 1996;94(suppl I):I-343-I-344. Abstract.
19. Roerdink F, Dijkstra J, Hartman G, Bolscher B, Scherphof G. The involvement of parenchymal, Kupffer and endothelial liver cells in the hepatic uptake of intravenously injected liposomes: effects of lanthanum and gadolinium salts. *Biochim Biophys Acta*. 1981;677: 79-89.
20. Chow DD, Essien HE, Padki MM, Hwang KJ. Targeting small unilamellar liposomes to hepatic parenchymal cells by dose effect. *J Pharmacol Exp Ther*. 1989;248:506-513.
21. Lund-Katz S, Phillips MC. Packing of cholesterol molecules in human low-density lipoprotein. *Biochemistry*. 1986;25:1562-1568.
22. Fiske CH, Subbarow Y. The colorimetric determination of phosphorus. *J Biol Chem*. 1924;66:375-400.
23. Anonymous. 1986 Report of the AVMA Panel on Euthanasia. *J Am Vet Med Assoc*. 1986;188:252-268.
24. Allain CC, Poon LS, Chan CS, Richmond W, Fu PC. Enzymatic determination of total serum cholesterol. *Clin Chem*. 1974;20: 470-475.
25. Sparks DL, Phillips MC. Quantitative measurement of lipoprotein surface charge by agarose gel electrophoresis. *J Lipid Res*. 1992;33: 123-130.
26. Reardon MF, Poapst ME, Uffelman KD, Steiner G. Improved method for quantitation of B apoprotein in plasma lipoproteins by electroimmunoassay. *Clin Chem*. 1981;27:892-895.
27. Kieft KA, Bocan TM, Krause BR. Rapid on-line determination of cholesterol distribution among plasma lipoproteins after high-performance gel filtration chromatography. *J Lipid Res*. 1991;32: 859-866.
28. Wolle S, Via DP, Chan L, Cornicelli JA, Bisgaier CL. Hepatic overexpression of bovine scavenger receptor type I in transgenic mice prevents diet-induced hyperbetalipoproteinemia. *J Clin Invest*. 1995;96:260-272.
29. Rea TJ, DeMattos RB, Pape ME. Hepatic expression of genes regulating lipid metabolism in rabbits. *J Lipid Res*. 1993;34: 1901-1910.
30. Pape ME, Melchior GW, Marotti KR. mRNA quantitation by a simple and sensitive RNase protection assay. *Genet Anal Tech Appl*. 1991;8:206-213.
31. Tall AR, Tabas I, Williams KJ. Lipoprotein-liposome interactions. *Methods Enzymol*. 1986;128:647-657.
32. Ishikawa TT, MacGee J, Morrison JA, Glueck CJ. Quantitative analysis of cholesterol in 5 to 20 microliters of plasma. *J Lipid Res*. 1974;15:286-291.
33. Klansek J, Yancey PG, St Clair RW, Fischer RT, Johnson WJ, Glick JM. Cholesterol quantitation by GLC: artifactual formation of short-chain steryl esters. *J Lipid Res*. 1995;36:2261-2266.
34. Markwell MA, Haas SM, Bieber LL, Tolbert NE. A modification of the Lowry procedure to simplify protein determination in membrane and lipoprotein samples. *Anal Biochem*. 1978;87: 206-210.
35. Takayama M, Itoh S, Nagasaki T, Tanimizu I. A new enzymatic method for determination of serum choline-containing phospholipids. *Clin Chim Acta*. 1977;79:93-98.
36. Glantz SA. *Primer of Biostatistics*. 3rd ed. New York, NY: McGraw-Hill, Inc; 1992.
37. Friedman M, Byers SO. Role of hyperphospholipidemia and neutral fat increase in plasma in the pathogenesis of hypercholesterolemia. *Am J Physiol*. 1956;186:13-18.
38. Tall AR, Green PH. Incorporation of phosphatidylcholine into spherical and discoidal lipoproteins during incubation of egg phosphatidylcholine vesicles with isolated high density lipoproteins or with plasma. *J Biol Chem*. 1981;256:2035-2044.
39. Rudel L, Deckelman C, Wilson M, Scobey M, Anderson R. Dietary cholesterol and downregulation of cholesterol 7-alpha hydroxylase

and cholesterol absorption in African green monkeys. *J Clin Invest.* 1994;93:2463-2472.
40. Xu G, Salen G, Shefer S, Ness GC, Nguyen LB, Parker TS, Chen TS, Zhao Z, Donnelly TM, Tint GS. Unexpected inhibition of cholesterol 7 alpha-hydroxylase by cholesterol in New Zealand White and Watanabe heritable hyperlipidemic rabbits. *J Clin Invest.* 1995;95:1497-1504.
41. Chonn A, Semple SC, Cullis PR. Separation of large unilamellar liposomes from blood components by a spin column procedure: towards identifying plasma proteins which mediate liposome clearance in vivo. *Biochim Biophys Acta.* 1991;1070:215-222.
42. Leichtner AM, Krieger M, Schwartz AL. Regulation of low density lipoprotein receptor function in a human hepatoma cell line. *Hepatology.* 1984;4:897-901.
43. Fuki IV, Preobrazhensky SN, Misharin AY, Bushmakina NG, Menschikov GB, Repin VS, Karpov RS. Effect of cell cholesterol content on apolipoprotein B secretion and LDL receptor activity in the human hepatoma cell line, HepG2. *Biochim Biophys Acta.* 1989;1001:235-238.
44. Bloch K. Some aspects of the control of lipid biosynthesis. *Adv Exp Med Biol.* 1975;60:1-12.
45. Edwards PA. Effect of plasma lipoproteins and lecithin-cholesterol dispersions on the activity of 3-hydroxy-3-methylglutaryl-coenzyme A reductase of isolated rat hepatocytes. *Biochim Biophys Acta.* 1975;409:39-50.
46. Breslow JL, Spaulding DR, Lothrop DA, Clowes AW. Effect of lipoprotein on 3-hydroxy-3-methylglutaryl coenzyme A (HMG CoA) reductase activity in rat liver cell culture: special suppressant effect of a lipoprotein isolated from hypercholesterolemic rat plasma. *Biochem Biophys Res Commun.* 1975;67:119-125.
47. Cooper AD. The regulation of 3-hydroxy-3-methylglutaryl coenzyme A reductase in the isolated perfused rat liver. *J Clin Invest.* 1976;57:1461-1470.
48. Dixon JL, Ginsberg HN. Regulation of hepatic secretion of apolipoprotein B-containing lipoproteins: information obtained from cultured liver cells. *J Lipid Res.* 1993;34:167-179.
49. Tanaka M, Otani H, Yokode M, Kita T. Regulation of apolipoprotein B secretion in hepatocytes from Watanabe heritable hyperlipidemic rabbit, an animal model for familial hypercholesterolemia. *Atherosclerosis.* 1995;114:73-82.
50. Shefer S, Nguyen LB, Salen G, Ness GC, Chowdhary HR, Lerner S, Batta AK, Tint GS. Differing effects of cholesterol and taurocholate on steady state hepatic HMG-CoA reductase and cholesterol 7 alpha-hydroxylase activities and mRNA levels in the rat. *J Lipid Res.* 1992;33:1193-1200.
51. Wisse E. An electron microscope study of the fenestrated endothelial lining of rat liver sinusoids. *J Ultrastruct Res.* 1970;31:125-150.
52. Fraser R, Dobbs BR, Rogers GW. Lipoproteins and the liver sieve: the role of the fenestrated sinusoidal endothelium in lipoprotein metabolism, atherosclerosis, and cirrhosis. *Hepatology.* 1995;21:863-874.
53. Pieters MN, Esbach S, Schouten D, Brouwer A, Knook DL, Van Berkel TJ. Cholesteryl esters from oxidized low-density lipoproteins are in vivo rapidly hydrolyzed in rat Kupffer cells and transported to liver parenchymal cells and bile. *Hepatology.* 1994;19:1459-1467.
54. Bjorkhem I, Andersson O, Diczfalusy U, Sevastik B, Xiu RJ, Duan C, Lund E. Atherosclerosis and sterol 27-hydroxylase: evidence for a role of this enzyme in elimination of cholesterol from human macrophages. *Proc Natl Acad Sci U S A.* 1996;91:8592-8596.
54a. Blomoff R, Helgerud P, Rasmussen M, Berg T, Norum KR. In vivo uptake of chylomicron [^{3}H]retinyl ester by rat liver: evidence for retinol transfer from parenchymal to nonparenchymal cells. *Proc Natl Acad Sci U S A.* 1982;79:7326-7330.
55. Wetterau JR, Jonas A. Effect of dipalmitoylphosphatidylcholine vesicle curvature on the reaction with human apolipoprotein A-I. *J Biol Chem.* 1992;257:10961-10966.
56. Williams KJ, Tall AR, Bisgaier C, Brocia R. Phospholipid liposomes acquire apolipoprotein E in atherogenic plasma and block cholesterol loading of cultured macrophages. *J Clin Invest.* 1987;79:1466-1472.
57. Bisgaier CL, Siebenkas MV, Williams KJ. Effects of apolipoproteins A-IV and A-I on the uptake of phospholipid liposomes by hepatocytes. *J Biol Chem.* 1989;264:862-866.
58. Quinet EM, Agellon LB, Kroon PA, Marcel YL, Lee YC, Whitlock ME, Tall AR. Atherogenic diet increases cholesteryl ester transfer protein messenger RNA levels in rabbit liver. *J Clin Invest.* 1990;85:357-363.
59. Whitlock ME, Swenson TL, Ramakrishnan R, Leonard MT, Marcel YL, Milne RW, Tall AR. Monoclonal antibody inhibition of cholesteryl ester transfer protein activity in the rabbit: effects on lipoprotein composition and high density lipoprotein cholesteryl ester metabolism. *J Clin Invest.* 1989;84:129-137.
60. Marotti KR, Castle CK, Murray RW, Rehberg EF, Polites HG, Melchior GW. The role of cholesteryl ester transfer protein in primate apolipoprotein A-I metabolism: insights from studies with transgenic mice. *Arterioscler Thromb.* 1992;12:736-744.
61. Marotti KR, Castle CK, Boyle TP, Lin AH, Murray RW, Melchior GW. Severe atherosclerosis in transgenic mice expressing simian cholesteryl ester transfer protein. *Nature.* 1993;364:73-75.
62. Hayek T, Masucci-Magoulas L, Jiang X, Walsh A, Rubin E, Breslow JL, Tall AR. Decreased early atherosclerotic lesions in hypertriglyceridemic mice expressing cholesteryl ester transfer protein transgene. *J Clin Invest.* 1995;96:2071-2074.
63. Constantinides P. Plaque fissures in human coronary thrombosis. *J Atheroscler Res.* 1966;61:1-17.
64. Davies MJ, Richardson PD, Woolf N, Katz DR, Mann J. Risk of thrombosis in human atherosclerotic plaques: role of extracellular lipid, macrophage, and smooth muscle cell content. *Br Heart J.* 1993;69:377-381.
65. Brown BG, Zhao XQ, Sacco DE, Albers JJ. Lipid lowering and plaque regression: new insights into prevention of plaque disruption and clinical events in coronary disease. *Circulation.* 1993;87:1781-1791.
66. Lesnik P, Rouis M, Skarlatos S, Kruth HS, Chapman MJ. Uptake of exogenous free cholesterol induces upregulation of tissue factor expression in human monocyte-derived macrophages. *Proc Natl Acad Sci U S A.* 1992;89:10370-10374.
67. Bottalico LA, Keesler GA, Fless GM, Tabas I. Cholesterol loading of macrophages leads to marked enhancement of native lipoprotein(a) and apoprotein(a) internalization and degradation. *J Biol Chem.* 1993;268:8569-8573.
68. Watson KE, Bostrom K, Ravindranath R, Lam T, Norton B, Demer LL. TGF-beta 1 and 25-hydroxycholesterol stimulate osteoblast-like vascular cells to calcify. *J Clin Invest.* 1994;93:2106-2113.
69. Williams KJ, Tabas I. The response-to-retention hypothesis of early atherogenesis. *Arterioscler Thromb Vasc Biol.* 1995;15:551-561.
70. Ludmer PL, Selwyn AP, Shook TL, Wayne RR, Mudge GH, Alexander RW, Ganz P. Paradoxical vasoconstriction induced by acetylcholine in atherosclerotic coronary arteries. *N Engl J Med.* 1986;315:1046-1051.
71. Rubba P, Mancini M. Lipid lowering treatment: effects on endothelial dysfunction. *Curr Opin Lipidol.* 1996;6:348-353.
72. Henry PD. Atherosclerosis, calcium, and calcium antagonists. *Circulation.* 1985;72:456-459.
73. Tulenko TN. Cholesterol enrichment of arterial smooth muscle cells promotes cell proliferation by induction of mitogen synthesis/release. *FASEB J.* 1994;8:A401. Abstract.
74. Bialecki RA, Tulenko TN, Colucci WS. Cholesterol enrichment increases basal and agonist-stimulated calcium influx in rat vascular smooth muscle cells. *J Clin Invest* 1991;88:1894-1900.
75. Stuart MJ, Gerrard JM, White JG. Effect of cholesterol on production of thromboxane B_2 by platelets in vitro. *N Engl J Med.* 1980;302:6-10.
76. Hochgraf E, Levy Y, Aviram M, Brook JG, Cogan U. Lovastatin decreases plasma and platelet cholesterol levels and normalizes elevated platelet fluidity and aggregation in hypercholesterolemic patients. *Metabolism.* 1994;43:11-17.
77. Opper C, Clement C, Schwarz H, Krappe J, Steinmetz A, Schneider J, Wesemann W. Increased number of high sensitive platelets in hypercholesterolemia, cardiovascular diseases, and after incubation with cholesterol. *Atherosclerosis.* 1995;113:211-217.
78. Notarbartolo A, Davi G, Averna M, Barbagallo CM, Ganci A, Giammarresi C, La Pianca FP, Patrono C. Inhibition of thromboxane biosynthesis and platelet function by simvastatin in type IIa hypercholesterolemia. *Arterioscler Thromb Vasc Biol.* 1995;15:247-251.

Exhibit F

SIGMA-ALDRICH

Material Safety Data Sheet

Date Printed: 01/09/2003
Date Updated: 09/01/2002
Version 1.30

Section 1 - Product and Company Information

Product Name PROPIDIUM IODIDE, 95%
Product Number 287075
Brand Aldrich Chemical

Company Sigma-Aldrich
Street Address 3050 Spruce Street
City, State, Zip, Country SAINT LOUIS, MO 63103 US
Technical Phone: 314 771 5765 **Emergency Phone:** 414 273 3850 Ext. 5996
Fax: 800 325 5052

Section 2 - Composition/Information on Ingredient

Substance Name	CAS #	SARA 313
PROPIDIUM IODIDE	25535-16-4	No

Formula C27H34N4.2I
Synonyms 3,8-Diamino-5-(3-(diethylmethylammonio)propyl)-6-phenylphenanthridinium diiodide, Propidium diiodide, Propidium iodide

Section 3 - Hazards Identification

Emergency Overview
Irritant.
Irritating to eyes, respiratory system, and skin.

HMIS Rating
Health: 2 Flammability: 0 Reactivity: 1

NFPA Rating
Health: 2 Flammability: 0 Reactivity: 1

For additional information on toxicity, please refer to Section 11.

S ction 4 - First Aid Measures

Oral Exposure
If swallowed, wash out mouth with water provided person is conscious. Call a physician.

Inhalation Exposure
If inhaled, remove to fresh air. If not breathing give artificial respiration. If breathing is difficult, give oxygen.

Dermal Exposure
In case of contact, immediately wash skin with soap and copious amounts of water.

Eye Exposure
In case of contact, immediately flush eyes with copious amounts of water for at least 15 minutes.

Section 5 - Fir Fighting Measures

Autoignition Temp: N/A

Extinguishing Media
Suitable
Water spray. Carbon dioxide, dry chemical powder, or appropriate foam.

Firefighting
Protective Equipment
Wear self-contained breathing apparatus and protective clothing to prevent contact with skin and eyes.
Specific Hazard(s)
Emits toxic fumes under fire conditions.

Section 6 - Accidental Release Measures

Procedure to be Followed in Case of Leak or Spill
Evacuate area.

Procedure(s) of Personal Precaution(s)
Wear respirator, chemical safety goggles, rubber boots, and heavy rubber gloves.

Methods for Cleaning Up
Sweep up, place in a bag and hold for waste disposal. Avoid raising dust. Ventilate area and wash spill site after material pickup is complete.

S ction 7 - Handling and Storage

Handling
User Exposure
Do not breathe dust. Avoid contact with eyes, skin, and clothing. Avoid prolonged or repeated exposure.

Storage
Suitable
Keep tightly closed. Store at 2-8°C (35.6-46.4°F). Store in the dark.

Special Requirements
Light sensitive Hygroscopic. Refrigerate.

Section 8 - Exposure Controls / PPE

Engineering Controls
Safety shower and eye bath. Mechanical exhaust required.

Personal Protective Equipment
Respiratory
Government approved respirator.
Hand
Compatible chemical-resistant gloves.
Eye
Chemical safety goggles.

General Hygiene Measures
Wash thoroughly after handling.

Section 9 - Physical/Chemical Properties

Appearance

Physical State	Color
Solid	Deep red

Molecular Weight:	668.41 AMU
pH	N/A
BP/BP Range	N/A
MP/MP Range	220 - 225 °C
Freezing Point	N/A
Vapor Pressure	N/A
Vapor Density	N/A
Saturated Vapor Conc.	N/A
SG/Density	N/A
Bulk Density	N/A
Odor Threshold	N/A
Volatile%	N/A
VOC Content	N/A
Water Content	N/A
Solvent Content	N/A
Evaporation Rate	N/A
Viscosity	N/A
Partition Coefficient	N/A
Decomposition Temp.	N/A
Flash Point °F	N/A
Flash Point °C	N/A
Explosion Limits	N/A
Flammability	N/A
Autoignition Temp	N/A
Solubility	N/A

N/A = not available

Section 10 - Stability and Reactivity

Stability
Stable
Stable.
Conditions of Instability
May decompose on exposure to light May decompose on exposure to moist air or water
Materials to Avoid
Strong oxidizing agents.

Hazardous Decomposition Products
Hazardous Decomposition Products
Carbon monoxide, Carbon dioxide, Nitrogen oxides, Hydrogen iodide.

Hazardous Polymerization
Hazardous Polymerization
Will not occur.

Section 11 - Toxicological Information

Route of Exposure
Skin Contact
Causes skin irritation.
Skin Absorption
May be harmful if absorbed through the skin.
Eye Contact
Causes eye irritation.
Inh lation
Material is irritating to mucous membranes and upper respiratory tract. May be harmful if inhaled.
Ingesti n
May be harmful if swallowed.

Signs and Symptoms of Exposure
To the best of our knowledge, the chemical, physical, and toxicological properties have not been thoroughly investigated.

RTECS Number: SF7949600

Toxicity Data

Subcutaneous - Mouse: 16 MG/KG (LD50)

Chronic Exposure - Mutagen
Result: Laboratory experiments have shown mutagenic effects.

Section 12 - Ecological Information

No data available.

Section 13 - Disposal Considerations

Appropriate Method of Disposal of Substance or Preparation
Contact a licensed professional waste disposal service to dispose of this material.
Dissolve or mix the material with a combustible solvent and burn in a chemical incinerator equipped with an afterburner and scrubber.
Observe all federal, state, and local environmental regulations.

Section 14 - Transport Information

DOT
Proper Shipping Name: None
Non-Hazardous for Transport: This substance is considered to be non-hazardous for transport.

IATA
Non-Hazardous for Air Transport: Non-hazardous for air transport.

S ction 15 - Regulatory Information

EU Additional Classification
Symbol of Danger: Xi
Indication of Danger
Irritant.
Risk Statements R: 36/37/38
Irritating to eyes, respiratory system, and skin.
Safety Statements S: 26
In case of contact with eyes, rinse immediately with plenty of water and seek medical advice.

US Classification and Label Text

Indication of Danger

Irritant.

Risk Statements

Irritating to eyes, respiratory system, and skin.

Safety Statements

In case of contact with eyes, rinse immediately with plenty of water and seek medical advice. Wear suitable protective clothing.

United States Regulatory Information

SARA Listed: No

Canada Regulatory Information

WHMIS Classification

This product has been classified in accordance with the hazard criteria of the CPR, and the MSDS contains all the information required by the CPR.

DSL: No

NDSL: No

Section 16 - Other Information

Disclaimer

For R&D use only. Not for drug, household or other uses.

Warranty

The above information is believed to be correct but does not purport to be all inclusive and shall be used only as a guide. Sigma-Aldrich Inc., shall not be held liable for any damage resulting from handling or from contact with the above product. See reverse side of invoice or packing slip for additional terms and conditions of sale.

Exhibit G

Applicant's Summary Of Differences Between The Prior Art And The Claimed Invention In 09/924,222

Hager (EP 0470437) (1992) • Hager discloses liposomes with a mean diameter between 50-180 nm and 70-130 nm. • Example 3 discloses liposomes with a mean diameter of 129 nm bound to propidiumiodide (a DNA marker and mutagen).	• Hager does not disclose a pharmaceutically acceptable liposome preparation having the claimed Gaussian distribution. • Example 3, the only disclosure of liposomes arguably within the claimed distribution, is not pharmaceutically acceptable.
Braun (EP 0461559) • Braun discloses unilamellar liposomes having an average diameter of: • 500 nm - "several microns" (p. 1, *l.* 15 English translation); • 60-500 nm (p. 1, *l.* 17 English translation); • 20-200 nm (p. 2, *l.* 12 English translation); • 200 nm (p. 11, *l.* 24 English translation); • below 200 nm (p. 10, *l.* 8 English translation); • 50-120 nm (p. 2, *l.* 25 English translation); • below 120 nm (p. 11, *ll.* 20-21 English translation); • 50-80 nm (p. 2, *l.* 26 English translation); • 20-50 nm (p. 1, *l.* 16 English translation); • 60 nm (p. 10, *l.* 11 English translation); • Braun teaches that the most effective liposomes are 60 nm (even though LDL increases). Data is limited to animal experiments.	• Braun does not disclose a pharmaceutically acceptable liposome preparation having the claimed Gaussian distribution.

Williams 1984 [Williams et al., *Intravenously Administered Lecithin Liposomes: A Synthetic Antiatherogenic Lipid Particle*, 27.3 PERSPECTIVES IN BIOLOGY AND MEDICINE 417-431 (1984)] • Williams 1984 discloses lecithin liposomes for mobilizing cholesterol and treating atherosclerosis having diameters of 30-60 nm (page 422, *ll.* 41-43 and page 425, *ll.* 41-44). Liposomes of 21-50 nm prepared by "vigorous agitation or, more effectively, by ultrasonic irradiation" are also disclosed (p. 419, *l.* 22).	• Williams 1984 does not disclose a pharmaceutically acceptable liposome preparation having the claimed Gaussian distribution.
Williams 1986 [Williams et al., *Uptake of Endogenous Cholesterol by a Synthetic Lipoprotein*, 875 BIOCHIMICA BIOPHYSICA ACTA 183-94 (1986)] • Williams 1986 discloses liposomes that are small unilamellar vesicles that are used in animals and *in vitro* human blood samples.	• Williams 1986 does not disclose a pharmaceutically acceptable liposome preparation having the claimed Gaussian distribution.
Williams 1988 [Williams et al., *Low Density Lipoprotein Receptor-Independent Hepatic Uptake of a Synthetic, Cholesterol-Scavenging Lipoprotein: Implications For The Treatment of Receptor-Deficient Atherosclerosis, 85 Proc. Natl. Acad. Sci. 242-46 (1988)*] • Williams 1988 discloses liposomes that are small unilamellar vesicles that are used in animals.	• Williams 1988 does not disclose a pharmaceutically acceptable liposome preparation having the claimed Gaussian distribution.

Rodrigueza '93 [Rodrigueza et al., *The Influence of Size and Composition On the Cholesterol Mobilizing Properties Of Liposomes In Vivo*, 1153 BIOCHIMICA BIOPHYSICA ACTA 9-19 (July 1993)] • Rodrigueza '93 discloses the use of liposomes with a mean diameter of 70±19 nm (LUV_{50}-unilamellar), 125±30 nm (LUV_{100}-unilamellar), and 237±90 nm (MLV_{400}-multilamellar) to mobilize cholesterol from the peripheral tissues of non-atherosclerotic mice.	• This article was authored by two of the inventors and published within one year of the priority date of the present application.
U.S. Patent No. 6,139,871] • Discloses compositions and methods using unilamellar liposomes having an average diameter of 100-150 nm for treating atherosclerosis.	• This patent is not prior art because the priority date of the present application is March 4, 1994.